



# Predictions of the reflectance factor of translucent layered dental resin composites using two-flux models: assessing the importance of the interface reflectance parameter

Vincent Duveiller, Emmanuel Kim, Marie Locquet, Arthur Gautheron, Raphael Clerc, Jean-Pierre Salomon, Mathieu Hébert

## ► To cite this version:

Vincent Duveiller, Emmanuel Kim, Marie Locquet, Arthur Gautheron, Raphael Clerc, et al.. Predictions of the reflectance factor of translucent layered dental resin composites using two-flux models: assessing the importance of the interface reflectance parameter. Colour and Visual Computing Symposium 2022, Sep 2022, Gjøvik, Norway. hal-03792814

**HAL Id: hal-03792814**

**<https://hal.science/hal-03792814>**

Submitted on 9 Dec 2022

**HAL** is a multi-disciplinary open access archive for the deposit and dissemination of scientific research documents, whether they are published or not. The documents may come from teaching and research institutions in France or abroad, or from public or private research centers.

L'archive ouverte pluridisciplinaire **HAL**, est destinée au dépôt et à la diffusion de documents scientifiques de niveau recherche, publiés ou non, émanant des établissements d'enseignement et de recherche français ou étrangers, des laboratoires publics ou privés.



Distributed under a Creative Commons Attribution 4.0 International License

# Predictions of the Reflectance Factor of Translucent Layered Dental Resin Composites Using Two-Flux Models: assessing the importance of the interface reflectance parameter

Vincent Duveiller<sup>1</sup>, Emmanuel Kim<sup>2</sup>, Marie Locquet<sup>2</sup>, Arthur Gautheron<sup>3</sup>, Raphaël Clerc<sup>1</sup>, Jean-Pierre Salomon<sup>4,5,6,7</sup> and Mathieu Hébert<sup>1</sup>

<sup>1</sup> Université de Lyon, UJM-Saint-Etienne, CNRS, Institut d'Optique Graduate School, Laboratoire Hubert Curien UMR 5516, F-42023, Saint-Etienne, France

<sup>2</sup> Institut d'Optique Graduate School, Saint-Etienne, France

<sup>3</sup> Université de Lyon, INSA-Lyon, Université Claude Bernard Lyon 1, UJM-Saint-Etienne, CNRS, Inserm, CREATIS UMR 5220, U1294, F-69621, Lyon France

<sup>4</sup> Faculté d'Odontologie de Nancy, Département des Dispositifs Médicaux et Biomatériaux Dentaires, Université de Lorraine, France

<sup>5</sup> Institut de Science des Matériaux de Mulhouse UMR 7361 CNRS, Université de Haute Alsace, France

<sup>6</sup> Université de Strasbourg, France

<sup>7</sup> Department of Restorative Dentistry, Division of Biomaterials and Biomechanics. Oregon Health and Science University, Portland, Oregon, USA

## Abstract

Two-flux models are practical tools for predicting the appearance of strongly scattering materials, but may fail to predict the spectral reflectance factor of translucent (i.e. weakly scattering) materials because of the simplifying assumptions upon which they are based. In a previous study, we showed how the internal reflectance at the interface of translucent layers, a parameter usually calculated assuming a Lambertian angular light distribution, can be adjusted in order to consider a directional light distribution, thus improving the predictive performance of the two-flux model applied to translucent dental resin composites. In this paper, we explore the dependence of this parameter on the layer's thickness and show how different values should be considered for accurately predicting the spectral reflectance factor of either thin or thick layers of translucent direct resin composites according to their thickness. We also extend the model to the layering procedure of resin with different levels of opacity which usually belong to the category of thick layers and show that the two-flux model can reach good prediction accuracy for their spectral reflectance factor.

## Keywords

translucent, Kubelka-Munk, four-flux, spectrophotometer, dental resin composite

## 1. Introduction

The appearance management of dental restorations opens up new prospects for the practice of dentists and manufacturers of dental materials, such as the development of materials which more faithfully mimic the optical characteristics of human enamel and dentin, the improvement of aesthetic quality of dental restorations, or in the long term, the use of 3D printers to make dental restorations, overall improving patient care.

However, dental materials, just as skin or many other biological tissues, are translucent, i.e., weakly scattering on an optical point of view [1,2]. This undermines simple flux transfer models, e.g., two-flux

---

The 11<sup>th</sup> Colour and Visual Computing Symposium, September 8–9, 2022, Gjøvik, Norway

EMAIL: vincent.duveiller@institutoptique.fr (A. 1); emmanuel.kim@institutoptique.fr (A. 2); marie.locquet@institutoptique.fr (A. 3); gautheron@creatis.insa-lyon.fr (A. 4); raphael.clerc@institutoptique.fr (A. 5); jpsalomon61@gmail.com (A. 6); mathieu.hebert@institutoptique.fr (A. 7)



© 2022 Copyright for this paper by its authors.

Use permitted under Creative Commons License Attribution 4.0 International (CC BY 4.0).

CEUR Workshop Proceedings (CEUR-WS.org)

[3,4,5] or four-flux [6,7] models, in their ability to predict the spectral reflectance factor, and consequently the color of dental materials under a certain lighting. While these models are well suited to the study of highly scattering materials such as paints [8,9] or textiles [10], they often fail in predicting accurately the reflectance factor of slices of translucent materials in which light can keep some directionality when crossing the material. Solving methods of the Radiative Transfer Equation [11-17] can overcome this issue, but they are ruled out because of the complex optical measurements required for their calibration which makes them unfit to use in an optical device intended for dentists. Hence, two-flux and four-flux models remain interesting for their ease of practical implementation, and their predictive performance should be sought to be improved with translucent materials.

The two-flux model is very easy to use and only requires two measurements for its calibration. According to this model, the optical characteristics of a given material are described by its spectral absorption coefficient  $K(\lambda)$ , its spectral scattering coefficient  $S(\lambda)$  and its refractive index  $n$ , often assumed to be 1.5 as in this study [18]. However, it only considers the propagation of a Lambertian diffuse flux inside the material, which is not consistent with reality. Indeed, measuring instruments based on a *directional-hemispherical* (or *hemispherical-directional* geometry), capture the exiting radiance at a specific angle (just as our eyes when observing a scene under diffuse light). Even if the object receives a Lambertian illumination, the flux reaching the sensor does not necessarily come from the whole hemisphere and is therefore not representative of the Lambertian flux inside the object. This is especially the case for non-scattering materials (e.g., a glass plate) for which the received flux only comes from one specific angle, or for translucent materials. For a highly scattering material, for which it can be assumed that the radiance captured by a detector in any direction is proportional to the exitance of the object, the two-flux model's assumptions apply. In a previous study [19], we showed that the internal reflectance at the material-air interfaces is a key parameter for the prediction accuracy of the reflectance and transmittance factors. For a thin slice of translucent dental resin composite, a better prediction accuracy is achieved when considering internal reflectances corresponding to directional light, as if the slice was a non-scattering plate. The accuracy should be improved with a four-flux model describing the propagation of both directional and diffuse light into the material. Proposed by Maheu *et al.* [6], the four-flux model describes the propagation of a directional flux, its forward and backward scattering, and the propagation of diffuse light, inside a layer. A material is optically characterized by four spectral parameters: its spectral absorption coefficient  $k(\lambda)$ , its spectral scattering coefficient  $s(\lambda)$ , the spectral forward scattering ratio  $\zeta(\lambda)$  and the spectral average path length parameter  $\varepsilon(\lambda)$ . Rozé *et al.* [20,21] updated the four-flux model with look-up tables enabling to use the asymmetry parameter of the Henyey-Greenstein scattering phase function [22] denoted  $g$ , instead of  $\zeta$  and  $\varepsilon$ .

Nevertheless, the four-flux model does not solve the issue of the angular distribution of diffuse light at the interfaces, from which the internal reflectance of the interface is computed. Indeed, two-flux and four-flux optical models assume that the angular distribution of diffuse light is Lambertian at both interfaces of the layer, whereas in a recent study, Gautheron *et al.* [23] showed that it is far from being Lambertian in thin or weakly scattering layers and is not necessarily equal at both interfaces.

Because of the diversity of clinical situations encountered by dentists, optical models predicting the color of dental materials must be accurate in various cases: for a single layer of material or layering of two different materials for a wide range of thicknesses.

Layering procedure of resin composites aims to use a first deep layer (with a so-called dentin or opaque composite which aims to mimic optical properties of dentin, namely high levels of opacity and chromaticity) with a second superficial layer (with a so-called enamel or translucent composite which aims to reproduce optical properties of enamel, namely high level of translucency, different levels of lightness and opalescence).

Mikhail *et al.* assessed the accuracy of the two-flux model for predicting the reflectance factor of dental resin composite samples in optical contact on drawdown cards for thicknesses ranging from 0.3 mm to 1.2 mm [18], and for layering of samples of a total thickness of approximately 4 mm [24]. Kristiansen *et al.* and Wang *et al.* assessed the color prediction capability of the two-flux model to predict the color of 1.0 mm thick dental ceramic samples on 5.0 mm samples [25,26].

In this paper, we study the two-flux and four-flux models' ability to predict the reflectance factor of samples of dental resin composites for different thicknesses, the ability of the two-flux model's matrix formalism to predict the reflectance factor of layered resin composites, and highlight the influence of

the internal reflectance at the interface parameter in the predictive performance of these models for thin samples and thick layered dental resin composites.

## 2. Materials and methods

This experiment was carried out with samples made of the Estelite Universal Flow Medium in A2 and OA2 shades (Tokuyama Company). In the Vita Classical colorimetric terminology of dental resin composites, the A2 shade is a light color with low chroma level, which aims to replace enamel. The OA2 shade corresponds to the same color, but is opaquer than the A2 shade. It aims to replace the dentin within the tooth, whose optical properties it imitates. Estelite Universal Flow is a direct light cured supra-nano filled resin composite. It contains spherical silica-zirconia filler (mean particle size: 200 nm), bis-GMA, Bis-MPEPP, TEGDMA, UMDA, Mequinol, Dibutyl hydroxyl toluene, and UV absorber. Batch numbers of A2 and OA2 shades are respectively 0503 and 7095. The Estelite Universal Flow Medium A2 material will be referred to as A2 and the Estelite Universal Flow Medium OA2 material will be referred to as OA2.

### 2.1. Samples preparation

For both shades A2 and OA2, eight flat cylindrical samples with different thicknesses were fabricated. The flowable dental resin was injected between two glass-slides, whose spacing is controlled with high precision wedges and defines the nominal thickness of the sample. Samples with thickness 0.4 mm, 0.5 mm, 0.8 mm, 1.0 mm, 1.2 mm, 1.5 mm, 1.6 mm, and 2.0 mm were made. The samples were light cured with a L.E.D. light curing unit (Radii Xpert, SDI company at 1500 mW/cm<sup>2</sup>) according to the curing scheme I.S.O. 4049:2009 (each sample was irradiated five times, 40 seconds each irradiation, at 12-3-6-9 o'clock positions and ending in the center of the sample). The sample diameter, determined by the volume of material deposited, is ranging from 20 mm to 22 mm. The thickness of each sample was measured with a precision micrometer as resin composites shrink during the curing process. Although the measured thicknesses were considered in the experiments, samples will be referred to by their nominal thickness for clarity. The fabricated samples are presented on Figure 1 and Figure 2.

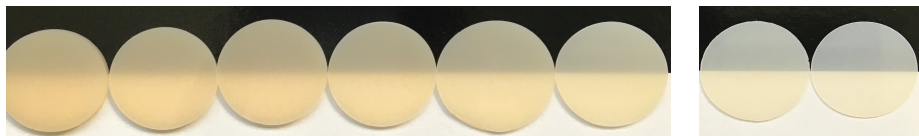


**Figure 1:** Samples of the Estelite Universal Flow Medium material shade A2 on a drawdown card (no optical contact). The picture is taken in daylight with an uncalibrated camera. Samples are sorted from the thickest on the left to the thinnest on the right: 2.0 mm, 1.6 mm, 1.5 mm, 1.2 mm, 1.0 mm, 0.8 mm, 0.5 mm and 0.4 mm.

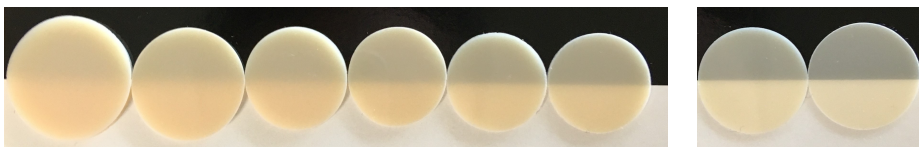


**Figure 2:** Samples of the Estelite Universal Flow Medium material shade OA2 on a drawdown card (no optical contact). The picture is taken in daylight with an uncalibrated camera. Samples are sorted from the thickest on the left to the thinnest on the right: 2.0 mm, 1.6 mm, 1.5 mm, 1.2 mm, 1.0 mm, 0.8 mm, 0.5 mm and 0.4 mm.

### 2.2. Optical measurements.

The Color i7 spectrophotometer from X-Rite (USA) was used to measure the spectral reflectance factor and transmittance factor of each sample. This device is based on the d:8° measuring geometry in reflectance mode and on the d:0° geometry in transmittance mode [27]. The highest possible illumination aperture of 17 mm was selected, while the smallest measuring aperture of 6 mm was selected in order to limit the edge-loss phenomenon, which is known to alter the measurement of translucent materials [28,29]. Measurements were performed from 400 nm to 750 nm by steps of 10 nm with a UV filter blocking wavelengths lower than 400 nm to prevent UV to visible fluorescence, which is not accounted for by the evaluated two-flux and four-flux optical models. Each measurement was repeated seven times and the average is calculated. To measure the reflectance factor of layered resin composites, each sample of the A2 shade was superimposed to several samples of the OA2 shade successively in order to create A2/OA2 couples of total thickness ranging from 1.0 mm to 4.0 mm. The optical contact was performed between samples using a clear immersion oil (Immersion Oil Type B from Cargille), which has a refractive index of 1.5180 at 546.1 nm. The A2/OA2 pairs evaluated are presented in table 1. The reflectance factor of an A2/OA2 couple being necessarily different from the reflectance factor of an OA2/A2 couple, the A2 samples (enamel-like shade) were always placed in front of the spectrophotometer, just as enamel is superposed to dentin in teeth. The spectral reflectance factor of each sample was also measured in optical contact on a black background (Byko-chart with  $L^* = 8.20$ ,  $a^* = -0.07$ ,  $b^* = 0.28$ ) and on a white background (Byko-chart with  $L^* = 91.5$ ,  $a^* = -0.46$ ,  $b^* = 4.65$ ).

**Table 1.**

Pairs of A2/OA2 samples evaluated for the prediction of their reflectance factor. The nominal thickness of each sample is given in mm.

A2 sample	OA2 sample
0.5	0.5
0.5	1.0
1.0	0.5
1.5	1.0
0.5	0.5
0.4	1.5
1.5	2.0
1.0	1.0
0.5	1.5
0.8	2.0
1.5	2.0
1.0	1.5
1.2	2.0
1.5	2.0
1.6	2.0
2.0	2.0

### 2.3. Experimental protocol.

To evaluate the capability of two-flux and four-flux optical models to predict the spectral reflectance and transmittance factors of translucent dental restorative materials, and the spectral reflectance factor of layered enamel/dentin resin layers of different thicknesses, the optical parameters of both A2 and OA2 materials according to the two-flux and four-flux models must be determined.

The inverse two-flux model provides close-form analytical formulae giving the material's spectral absorption coefficient  $K(\lambda)$  and spectral scattering coefficient  $S(\lambda)$  as functions of the measured spectral reflectance and transmittance factors, by assuming that the refractive index of the material is known (we assume  $n = 1.5$ ), and the thickness  $h$  of the sample under study is known as well.  $K$  and  $S$  coefficients

can be extracted for each wavelength either from the measured reflectance and transmittance factors of one sample, or from the reflectance factor measurements of the sample in optical contact against a black and a white background (with different sets of analytical formulae for each method). These two methods were implemented, and the method requiring reflectance and transmittance factor measurements for calibration is denoted the “2F-RT” model while the method requiring reflectance factor measurements on a black and on a white background for calibration is denoted the “2F-Rbw” model. In these two formalisms, the internal reflectance of the interface, denoted  $r_i$ , is involved. This parameter is calculated using eq. 1.

$$r_i = \int_{\theta=0}^{\pi/2} R_{21}(\theta) L(\theta) \sin(2\theta) d\theta / \int_{\theta=0}^{\pi/2} L(\theta) \sin(2\theta) d\theta, \quad (1)$$

where  $R_{21}$  is the material-air Fresnel reflectance and  $L(\theta)$  the outgoing radiance at the interface within a cone. Usually, one can assume that the radiance incident at the interfaces and reaching the sensor is Lambertian. In this case,  $L(\theta)$  is a constant and  $r_i$  is calculated by integrating the Fresnel reflectance over the hemisphere [30] as in eq. 2. For  $n = 1.5$ ,  $r_i = 0.5963$ .

$$r_i = \int_{\theta=0}^{\pi/2} R_{21}(\theta) \sin(2\theta) d\theta, \quad (2)$$

This value is used in the 2F-RT and 2F-Rbw models. In the latter, the white background being highly scattering, justifies the assumption of a uniform radiance falling on the interface.

We also implemented the two-flux reflectance/transmittance model, but this time assuming that the light falling on the interfaces and reaching the sensor is mainly directional (as in a non-scattering glass plate). In this case, the Fresnel reflectance is not integrated over the hemisphere for the calculation of  $r_i$ , which gives  $r_i = 0.04$  at normal incidence for  $n = 1.5$ . This model is denoted the “dir2F-RT” model.

In contrast with two-flux models, four-flux models cannot be easily inversed. Therefore, a fitting algorithm based on the *fmincon* Matlab® solver was implemented in order to minimize the root mean square difference between the predicted and measured reflectance/transmittance factors with respect to the model’s parameters. The four-flux model was implemented according to the formalism proposed by Rozé *et al.* [20,21] (denoted “Rozé4F-RT”), and also according to the formalism proposed by Eymard *et al.* [31] (denoted “Eymard4F-RT”). Compared to the four-flux as generalized by Maheu *et al.* [6], Rozé *et al.* calculated look-up tables enabling to use the asymmetry parameter of the Henyey-Greenstein phase function [22] denoted  $g$  as a fitting parameter instead of the forward scattering ratio  $\zeta$  and the average path length parameter  $\varepsilon$ , reducing the number of unknown from 4 to 3. Therefore, the refractive index can be used as a fourth fitting parameter instead of considering  $n = 1.5$ . Eymard’s four-flux model uses the Rozé4F-RT formalism, but considers the  $g$  parameter to calculate the internal reflectance at the interfaces of the layer (see eq. 3).

$$r_i = \int_{\theta=0}^{\pi/2} R_{21}(\theta) P_{HG}(g, \theta) \sin(2\theta) d\theta / \int_{\theta=0}^{\pi/2} P_{HG}(g, \theta) \sin(2\theta) d\theta \quad (3)$$

where  $P_{HG}$  is the Henyey-Greenstein phase function. This enables to use  $r_i$  as an indirect wavelength dependent fitting parameter for each material accounting for scattering anisotropy at the interfaces instead of considering a Lambertian angular light distribution, as it is done in the Rozé4F-RT model.

The parameters of the five aforementioned models are extracted using measurements of one sample with thickness  $h$  called *calibration sample*, and are assumed constant regardless of the thickness of the sample. Once calibrated, each model is used to predict the spectral reflectance and transmittance factors of other samples with different thicknesses. The spectral reflectance factor of stacks of samples is also predicted using the matrix formalism of the two-flux model. The prediction error is evaluated by calculating the color distance between measured and predicted spectra according to the perceptually stable CIEDE2000 color distance metric. Measured and predicted spectra are converted into CIE 1931 XYZ tristimulus values considering the color matching functions of the 2° standard observer and a D65 power spectral distribution as illuminant [32]. XYZ tristimulus values are then converted into the CIE 1976  $L^*a^*b^*$  color space by considering a perfect white diffuser under illuminant D65 as white reference for the chromatic adaptation. To assess the validity of predictions, the notions of *perceptibility threshold* and *acceptability threshold*, developed in [33-36] for dental resin composites and ceramics,

are considered. The perceptibility threshold corresponds to the color distance below which most human observers cannot distinguish two colors. It is evaluated between 0.8 and 1.3 CIEDE2000 units depending on the study. The acceptability threshold corresponds to the color distance under which two colors can be distinguished, but the color difference is deemed acceptable by most observers. It is evaluated between 1.8 and 2.25 CIEDE2000 units depending on the study.

### 3. Predictive performance of two-flux and four-flux models

The *2F-RT*, *dir2F-RT*, *2F-Rbw*, *Rozé4F-RT* and *Eymard4F-RT* models were applied to both A2 and OA2 samples and their predictive performance was assessed.

#### 3.1. Prediction of single samples.

Figure 3 (resp. Figure 4) shows the prediction accuracy for the reflectance and transmittance factors of A2 (resp. OA2) shade predicted by the *2F-RT*, *dir2F-RT*, *2F-Rbw*, *Rozé4F-RT* and *Eymard4F-RT* optical models when the calibration sample is the sample with 1.2 mm thickness (Figure 3a, resp. Figure 4a) and when it is the sample with 2.0 mm thickness (Figure 3b, resp. Figure 4b). In each graphic, the lower grey rectangle represents the perceptibility threshold and the upper grey rectangle represents the acceptability threshold.

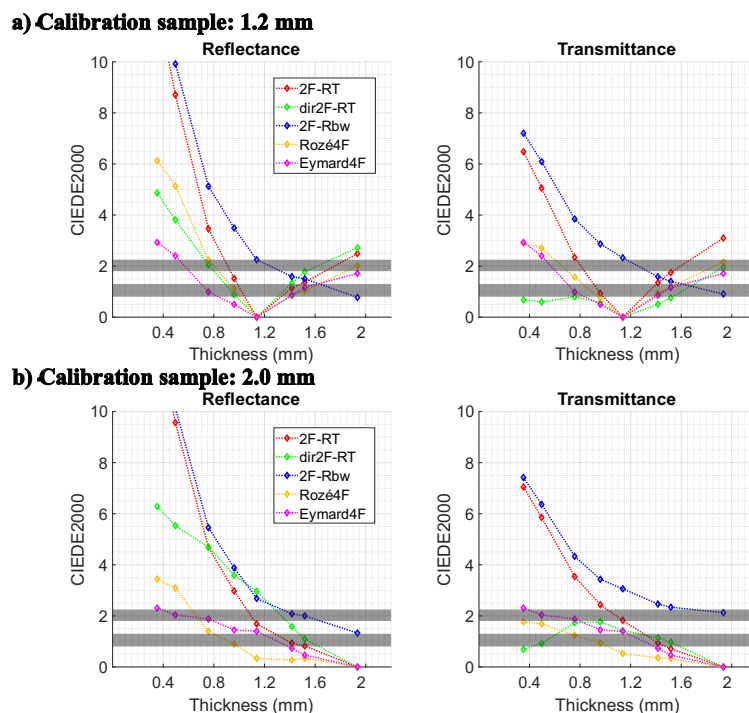


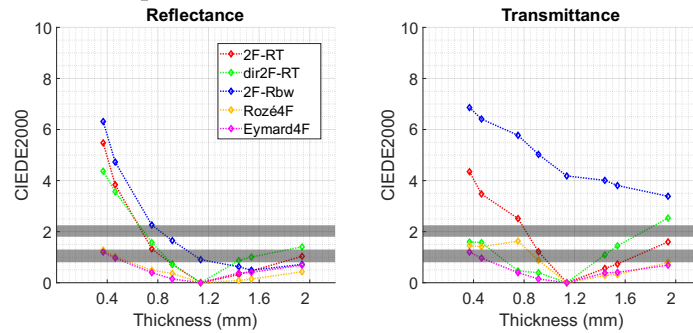
**Figure 3:** Deviation between measured and predicted reflectance factors (left graphic) and transmittance factors (right graphic) expressed in CIEDE2000 color distance units, for samples of the Estelite Universal Flow Medium material, A2 shade. (a) The sample with thickness 1.2 mm is used for the calibration of the models. (b) The sample with thickness 2.0 mm is used for the calibration of the models.

Notice that the color distance between the predictions and the measurements reaches 0 for the thickness of the calibration sample except for the *2F-Rbw* model. This is because the *2F-RT*, *dir2F-RT*, *Rozé4F-RT* and *Eymard4F-RT* models were calibrated using reversible protocols aimed at finding the parameters that minimize the color deviation for this sample, while the *2F-Rbw* model predicting the reflectance and transmittance factors was calibrated using reflectance factor measurements performed



on drawdown cards (which minimizes the color deviation of predictions made on drawdown cards rather than reflectance/transmittance factor predictions).

**a) Calibration sample: 1.2 mm**



**b) Calibration sample: 2.0 mm**

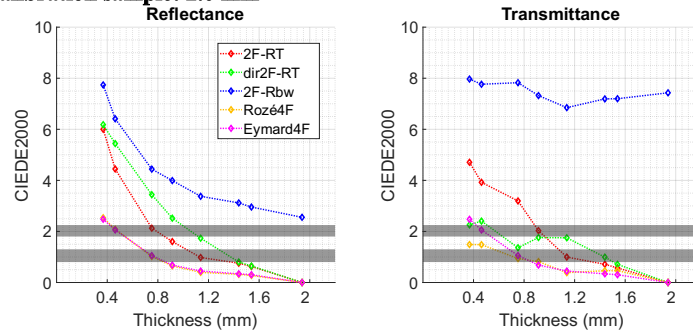


**Figure 4:** Deviation between measured and predicted reflectance factors (left graphic) and transmittance factors (right graphic) expressed in CIEDE2000 color distance units, for samples of the Estelite Universal Flow Medium material, OA2 shade. (a) The sample with thickness 1.2 mm is used for the calibration of the models. (b) The sample with thickness 2.0 mm is used for the calibration of the models.

Generally, the five optical models are more accurate for predicting the spectral reflectance factor of the OA2 shade than the A2 shade. Indeed, OA2 shade, being opaquer and less translucent, is more in line with the simplifying assumptions of two-flux and four-flux models.

For thicker samples, we expect the assumption of the Lambertian angular distribution of light at the interface and then reaching the sensor to be more valid than for thin samples, since light is necessarily more and more diffuse as it crosses the translucent layer. However, extracting the optical parameters from the thickest sample does not improve the prediction accuracy of two-flux models: the color distance increases rapidly when the thickness of the evaluated sample differs from the thickness of the calibration sample. This shows that the two-flux model, as we implemented it, is not suited for predicting the spectral reflectance factor of thin resin composites of dental biomaterials. Nonetheless, the dir2F-RT model accurately predicts the spectral transmittance factor of most samples of A2 and OA2 shades.

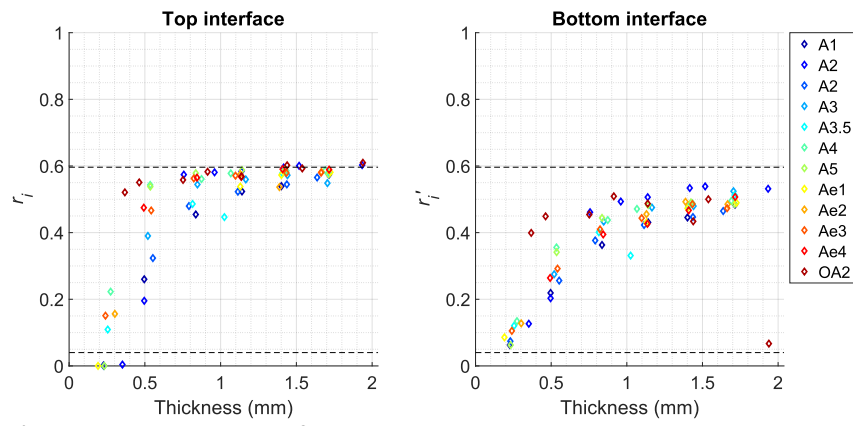
The four-flux models are generally more accurate than the two-flux models for predicting the spectral reflectance factor of A2 and OA2 samples. The Eymard4F-RT model, using  $r_i$  as an indirect fitting parameter, is more precise than the Rozé4F-RT model in most cases, especially for thin samples, which shows the importance of adapting the value of the internal reflectance at the interfaces. Nonetheless, even four-flux models do not provide acceptable reflectance factor predictions for the thinnest samples, which shows that work is still needed to address the physical issues posed by samples with thicknesses lower than 0.4 mm.

### 3.2. Fitting the interfaces' internal reflectance.

We have observed that the value of  $r_i$  has a major influence in the accuracy of two-flux and four-flux models. However, means to account for the specific angular light distribution at the interfaces are scarce, as spectrophotometers used in conjunction with two-flux and four-flux models do not permit to



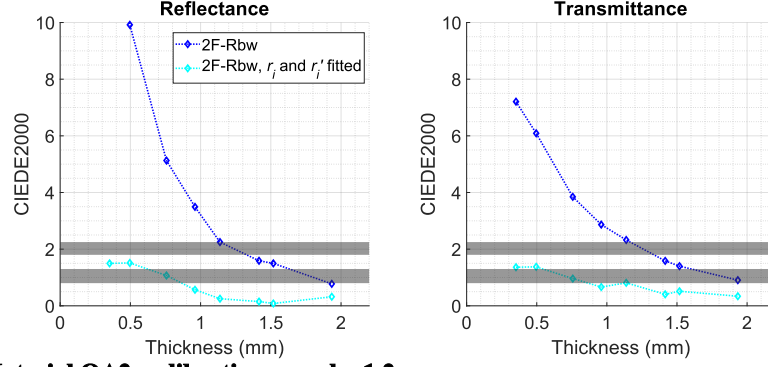
measure it. In a recent paper, Gautheron *et al.* [23] have shown the dependence of the internal reflectance at the top (denoted  $r_i$ ) and bottom (denoted  $r_i'$ ) interfaces of layers of translucent materials with respect to their optical properties (namely, its absorption and scattering coefficients, asymmetry parameter of the scattering phase function and refractive index) and their thickness. In an attempt to evaluate the internal reflectance at both top and bottom interfaces, we implemented an optimization algorithm to fit the reflectance and transmittance factors predicted by 2F-Rbw model to measurements, with  $r_i$  and  $r_i'$  as fitting parameter. As the white background is highly scattering, we assume that the  $r_i$  value 0.5963 used to extract the absorption and scattering coefficients of the 2F-Rbw model is the most valid in this case. Once the absorption  $K$  and scattering  $S$  parameters are extracted, the reflectance and transmittance factors are fitted with  $r_i$  and  $r_i'$  as free parameters. This experiment was repeated with many other dental resin composites at our disposal. The extracted  $r_i$  and  $r_i'$  parameters are presented on Figure 5. Values of  $r_i$  and  $r_i'$  show a strong dependence to the thickness of the sample from which they are extracted. Furthermore, their distribution seems consistent with the modelling presented by Gautheron *et al.* [23].



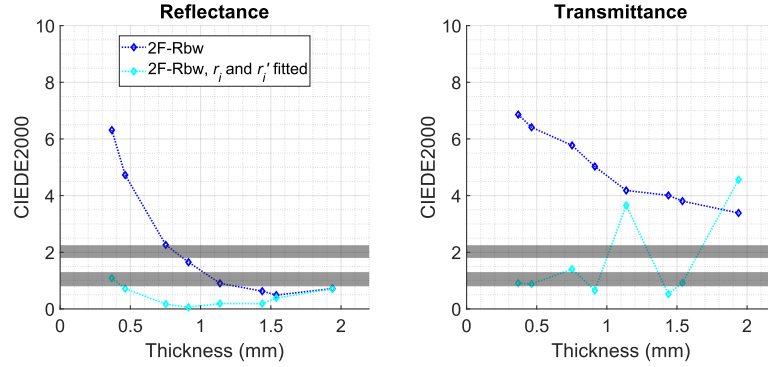
**Figure 5:**  $r_i$  and  $r_i'$  parameters extracted from numerous translucent dental biomaterials.

Figure 6a (resp. Figure 6b) shows the improvement in prediction accuracy of the 2F-Rbw model enabled by the fitting of  $r_i$  and  $r_i'$ . Note that Figure 6 should not be compared with Figure 3 and 4 but it shows that a thickness dependent value for  $r_i$  and  $r_i'$  improves the accuracy of the model.

**a) Material A2, calibration sample: 1.2 mm**



**b) Material OA2, calibration sample: 1.2 mm**



**Figure 6:** New prediction accuracy (cyan curves) of the 2F-Rbw model with  $r_i$  and  $r_i'$  fitted compared to the previous predictive performance (blue curves). The calibration sample has a 1.2 mm thickness. (a) A2 Material. (b) OA2 Material.

### 3.3. Prediction of layered samples.

Finally, we implemented the matrix formalism of the two-flux model, which enables to predict the spectral reflectance factor of layered resin composites according to the 2F-RT, dir2F-RT, and 2F-Rbw formalisms. The CIEDE2000 values assessing the deviations between the predictions and the measurements are presented in Figure 7.

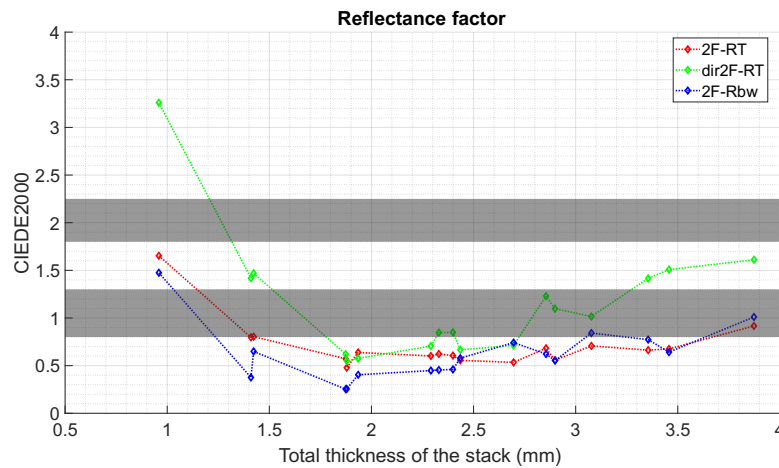


**Figure 7:** Deviation between measured and predicted reflectance factors expressed in CIEDE2000 color distance units, for A2/OA2 layered samples of the Estelite Universal Flow Medium material. The A2 and OA2 samples with thickness 1.0 mm are used for the calibration of the 2F-Rbw model while A2 and OA2 samples with thickness 2.0 mm are used for the calibration of the 2F-RT and dir2F-RT models.

The A2 and OA2 samples with thickness 1.0 mm were used to calibrate the 2F-Rbw model, while the A2 and OA2 samples with thickness 2.0 mm were used to calibrate the 2F-RT and dir2F-RT models. These calibration samples enable the best predictive performance for each model on average.

In contrast with the previous observations on thinner samples, the 2F-Rbw is the most accurate model. In this situation, the A2 samples are placed in optical contact against the OA2 sample, an opaquer (although still translucent) white background. Thus, optical parameters of the A2 and OA2 samples extracted with the 2F-Rbw model are necessarily closer to this case than the optical parameters extracted from reflectance and transmittance factor measurements, which partly explains the good predictive performance of this model. However, the 2F-RT model being almost as accurate as the 2F-Rbw model, and the dir2F-RT being the least accurate, indicates that the assumption of a Lambertian angular light distribution at both interfaces of the stack generally applies, which justifies using  $r_i = 0.5963$  in this case.

## 4. Conclusions

We implemented five different flux transfer models (two-flux and four-flux models) and analyzed their predictive performance for the reflectance and transmittance factors of samples with different, but relatively low, thicknesses. While two-flux models generally fail to predict the reflectance factor below the perceptibility threshold, we observe that the value of the internal reflectance of the bordering interfaces,  $r_i$ , plays a significant role in their respective prediction accuracy. Four-flux models, especially Eymard's model, were much more accurate than two-flux models but their prediction accuracy for the thinnest samples must still be improved. These results indicate that when the measurements are based on a geometry where the incident light or the captured light is directional (directional-hemispherical or hemispherical-directional geometry), which is almost always the case in practice, the light that is received by the sensor cannot be assumed perfectly diffuse (i.e., Lambertian) at any depth within the layer, in particular at the bordering interfaces. Consequently, the internal reflectance of the interface is different from the value 0.5963 that we would have with perfectly diffuse light in materials of refractive index 1.5.

By fitting the internal reflectance of the top and bottom interfaces with an optimization algorithm based on the two-flux model and repeating this operation with many different dental resin composites, we clearly observe that the optimal internal reflectance values vary with the sample thickness. This corroborates the idea that the angular distribution of light propagating into the material and falling on the interfaces before reaching the sensor is not uniform (i.e., non-Lambertian).

However, when thicker layered translucent resin composites are considered, the 2F-RT and 2F-Rbw models were found accurate enough at predicting their reflectance factor. The samples are thick enough in this case to strongly scatter light and meet the assumption that the light captured by the sensor is representative of the whole Lambertian light that propagates into the sample. It is also consistent with already published studies which are focused on similar types of translucent dental materials for thicknesses greater than 4 mm [24-26].

## 5. Acknowledgments

This work has been funded by a public grant from the French National Research Agency (ANR) under the "France 2030" investment plan, which has the reference EUR MANUTECH SLEIGHT - ANR-17-EURE-0026. It is also supported by LABEX PRIMES (ANR-11-LABX-0063) of Université de Lyon, within the program "Investissements d'Avenir" (ANR-11-IDEX-0007) operated by the French National Research Agency (ANR) and carried out within the framework of France Life Imaging (ANR-11-INBS-0006).

## 6. References

- [1] S. L. Jacques, Optical properties of biological tissues: a review, *Phys. Med. Biol.* 58 (2013): R37-R61.

- [2] X. Hu, Translucency estimation for thick pigmented maxillofacial elastomer, *Journal of Dentistry* 39S (2011): e2-e8.
- [3] P. Kubelka, M. Munk, Ein Beitrag zur Optik der Farbanstriche, *Zeitschrift für technische Physik* 23 (1931): 593-601.
- [4] P. Kubelka, New contributions to the optics of intensely light-scattering material, part I, *J. Opt. Soc. Am. A* 38 (1948): 448-457.
- [5] P. Kubelka, New contributions to the optics of intensely light-scattering material, part II: Non-homogeneous layers, *J. Opt. Soc. Am. A* 44 (1954): 330-335.
- [6] B. Maheu, J. N. Letoulouzan, G. Gouesbet, Four-flux models to solve the scattering transfer equation in terms of Lorenz-Mie parameters, *Appl. Opt.* 23(19) (1984): 3353-3362.
- [7] B. Maheu, G. Gouesbet G, Four-flux models to solve the scattering transfer equation: special cases, *Appl. Opt.* 25(7) (1986): 1122-1128.
- [8] R. S. Berns, M. Mohammadi, Single-Constant Simplification of Kubelka-Munk Turbid Media Theory for Paint Systems – A Review, *Color Res Appl* 32(3) (2007): 201-207.
- [9] Y. Zhao, R. S. Berns, Predicting the spectral reflectance factor of translucent paints using Kubelka-Munk turbid media theory: Review and evaluation, *Color Res Appl* 34(6) (2009): 417-431.
- [10] A. Moussa, Textile color formulation using linear programming based on Kubelka-Munk and Duncan theories, *Color Res Appl* 46(5) (2021): 1046-1056.
- [11] S. Chandrasekhar, *Radiative Transfer*, Dover Publication Inc., New York, 1960.
- [12] A. Ishimaru, *Wave propagation and scattering in random media*, volume 2, Academic press, New York, 1978.
- [13] K. Stamnes, S. C. Tsay, W. Wiscombe, K. Jayaweera, Numerically stable algorithm for discrete-ordinate-method radiative transfer in multiple scattering and emitting layer media, *Appl. Opt.* 27 (1988): 2502-2510.
- [14] M. Elias, G. Elias, New and fast calculation for incoherent multiple scattering, *J. Opt. Soc. Am. A*, 19 (2002): 894-905.
- [15] S. A. Prahl, *Light transport in tissues*. Ph.D. thesis, University of Texas, USA, 1988.
- [16] H. C. Van de Hulst H. C, *Multiple Light Scattering*, Academic Press, New York, 1980.
- [17] Q. Fang, D. Boas, Monte Carlo Simulation of Photon Migration in 3D Turbid Media Accelerated by Graphics Processing Units, *Opt. Express* 17 (2009): 20178-20190.
- [18] S. S. Mikhail, S. S. Azer, W. M. Johnston, Accuracy of Kubelka-Munk reflectance theory for dental resin composite material, *Dent. Mat.* 28 (2012): 729-735.
- [19] V. Duveiller, L. Gevaux, R. Clerc, J-P. Salomon, M. Hébert, Reflectance and transmittance of flowable dental resin composite predicted by the two-flux model: on the importance of analyzing the effective measurement geometry, in: *Proceedings of the 28<sup>th</sup> Color Imaging Conference*, Society for Imaging Science and Technology, 2020, pp. 313-320.
- [20] C. Rozé, T. Girasole, A-G. Tafforin, Multilayer four-flux model of scattering, emitting and absorbing media, *Atmospheric Environment* 35 (2001): 5125-5130.
- [21] C. Rozé, T. Girasole, G. Gréhan, G. Gouesbet, B. Maheu, Average crossing parameter and forward scattering ratio values in four-flux model for multiple scattering media, *Optics Communications* 194 (2001): 251-263.
- [22] L. G. Henyey, J. L. Greenstein, Diffuse Radiation in the galaxy, *The Astrophysical Journal* 93 (1941): 70-83.
- [23] A. Gautheron, R. Clerc, V. Duveiller, L. Simonot, B. Montcel, M. Hébert, Light scattering in translucent layers: angular distribution and internal reflections at flat interfaces, in *Proceedings of the IS&T International Symposium on Electronic Imaging 2022*, Society for Imaging Science and Technology, pp.221-1–221-6.
- [24] S. S. Mikhail, W. M. Johnston, Confirmation of theoretical colour predictions for layering dental composite materials, *Journal of Dentistry* 42(4) (2014): 419-424.
- [25] J. Kristiansen, M. Sakai, J. Da Silva, M. Gil, S. Ishikawa-Nagai, Assessment of a prototype computer colour matching system to reproduce natural tooth colour on ceramic restorations, *Journal of Dentistry* 39(Suppl. 3) (2011): e45-e51.
- [26] J. Wang, J. Lin, M. Gil, A. Seliger, J. D. Da Silva, S. Ishikawa-Nagai, Assessing the accuracy of computer color matching with a new dental porcelain shade system, *Journal of Prosthetic Dentistry* 111(3) (2014): 247-253.

- [27] CIE: Absolute methods for reflection measurements, CIE Technical Report, 1979.
- [28] W. M. Johnston, N. S. Hesse, B. K. Davis, R. R. Seghi, Analysis of edge-losses in reflectance measurements of pigmented maxillofacial elastomer, *Journal of Dental Research* 75(2) (1996): 752-760.
- [29] L. Gevaux, L. Simonot, R. Clerc, M. Gerardin, M. Hébert, Evaluating edge loss in the reflectance measurement of translucent materials, *Appl. Opt.* 59(28) (2020): 8939-8950.
- [30] D. B. Judd, Fresnel reflection of diffusely incident light, *J. Natl. Bur. Standards* 29 (1942): 329-332.
- [31] J. Eymard, R. Clerc, V. Duveiller, B. Commault, M. Hébert, Solar Energy Materials and Solar Cells Characterization of UV – Vis – NIR optical constants of encapsulant for accurate determination of absorption and backscattering losses in photovoltaics modules, *Solar Energy Materials and Solar Cells* 240 (2022): 11717.
- [32] CIE: Colorimetry, CIE Technical report, 3<sup>rd</sup> Ed., 1998.
- [33] R. Ghinea, M. M. Pérez, L. J. Herrera, M. José Rivas, A. Yebra, R. D. Paravina, Color difference thresholds in dental ceramics, *Journal of Dentistry* 38s (2010): e-57 – e-64.
- [34] R. D. Paravina, R. Ghinea, L. J. Herrera, A. D. Bona, C. Igiel, M. Linninger, M. Sakai, H. Takahashi, E. Tashkandi, M. M. Pérez, Color difference thresholds in dentistry, *Journal of Esthetic and Restorative Dentistry* 27(S1) (2015): S1-S9.
- [35] R. D. Paravina, M. M. Pérez, R. Ghinea, Acceptability and perceptibility thresholds in dentistry: A comprehensive review of clinical and research applications, *Journal of Esthetic and Restorative Dentistry* 31(2) (2019): 103-112.
- [36] J. A. Medeiros, O. E. Pecho, M. M. Pérez, F. Carrillo-Pérez, L. J. Herrera, A. Della Bona, Influence of background color on color perception in dentistry, *Journal of Dentistry* 108 (2021).